Modeling the lithium loop in a liquid metal pool-type divertor

Modeling the Lithium Loop in the DTT Liquid Metal Divertor

G. F. Nallo[a], S. Carli[a], G. Caruso[b], F. Crisanti[c], G. Mazzitelli[c], L. Savoldi[a], F. Subba[a], R. Zanino[a]

[a]*NEMO group, Dipartimento Energia, Politecnico di Torino, Torino, Italy*
[b]*Università degli Studi di Roma "La Sapienza", Roma, Italy*
[c]*ENEA Frascati, Italy*

Solutions for the steady-state power exhaust problem in future fusion reactors (e.g. DEMO) are neither provided by present experiments nor will be by ITER, because the expected heat fluxes, as well as the level of neutron irradiation, will be much higher. Dedicated work packages are being devoted to this problem within EUROfusion and even a dedicated facility (the Divertor Tokamak Test - DTT) is being proposed in Italy. Among the possible solutions to the problem, a liquid metal (LM) divertor was proposed more than 20 years ago. The particularly attractive feature of this solution is the absence of damage to the wall, even in the case of large heat fluxes, thanks to the high latent heat of evaporation and to the liquid nature of the wall, which can be constantly replenished. The present work aims at developing a simple model of the LM loop including the most important physical phenomena and allowing to roughly determine the operating range of the system, in terms of surface temperatures and vapor pressures. This work therefore sets the basis for the conceptual design of a LM divertor for the DTT facility. The preliminary model has been set up including the incoming plasma heat load and a basic treatment of the interactions of Li vapor with the plasma. The reduction of the Li vapor efflux due to ionization by the plasma is also taken into account. The model includes two chambers: a first divertor box, the evaporation chamber (EC), is open towards a second divertor box, the differential chamber (DC), which is in turn connected to the main plasma chamber (MC).
The model is used to study the effectiveness of the LM vapor in radiating isotropically the parallel heat flux incoming in the divertor. The results indicate that the presence of the DC allows a significant reduction of the Li vapor efflux towards the MC, which in turn would imply a lower contamination of the core plasma. Future studies will include a capillary-porous structure (CPS) coating of the internal surfaces of the divertor and a 2D approach to both plasma and Li vapor modeling.

Keywords: Plasma Exhaust, Divertor, Lithium, SOL, DTT

1. Introduction

Safe power exhaust, even in steady state, is one of the major issues in fusion reactors and a potential show-stopper towards the production of the first kWh from the fusion energy source, which the EU roadmap [1] has set as the major target for its DEMO reactor in 2050. The power produced by deuterium-tritium reactions in the alpha particles channel may be partly -- more or less isotropically -- radiated, but the rest reaches the plasma-facing components (PFCs) in the strongly anisotropic channel of plasma advection-conduction. This leads to high particle and heat fluxes, because of the relatively small wetted areas associated with the thin scrape-off layer (SOL) predicted in future machines, affecting not only the PFCs lifetime but also the core plasma purity (measured by the Z_{eff} parameter), because of sputtering.

In ITER, the control of the steady-state peak heat load q_{peak} below 10 MW/m^2 on the PFCs, as well as of the Z_{eff}, relies on a single-null divertor with W target and on the Be first wall (FW), combined with detached plasma operation and seed impurity puffing [2, 3]. Even if this complex combination of conditions should be confirmed experimentally in ITER, extrapolation to DEMO is not automatically guaranteed. Furthermore, as the increase in size from ITER to DEMO is much smaller than the increase in the design thermal power to be produced by the two machines, in DEMO it will be even more difficult to meet the technological constraints on q_{peak} related to the use of a solid divertor.
Among the risk-mitigation strategies currently foreseen, the one especially relevant for the present work is the liquid metal (LM) divertor [4]: the LM evaporation, together with the plasma cooling by interactions with the LM vapor, could in principle guarantee the exhaust of hundreds of MW/m^2, with much more limited, if any, damage to the target than the solid target option, and consequent increase of the divertor lifetime.

Possible LM choices include in the first place Li [2], which will be considered here, but also others, e.g. Sn. As to the nature of the LM target, different options are being considered, ranging in complexity from a simple pool to a moving liquid film, to the use of a so-called capillary porous structure (CPS) [4], recently tested on the liquid Li limiter (LLL) in FTU [5]. While the CPS should guarantee, better than other solutions, the avoidance of splashing phenomena with generation of LM droplets, which could easily compromise the plasma purity, we will refer in the present work to the simpler case of a LM pool without CPS and without external (pumped) circulation of the LM.

In the EU, significant attention is being given to these problems within the EUROfusion Work Packages DTT1 and DTT2. DTT is also the name of an Italian proposal for a machine entirely devoted to the issues of power exhaust and Z_{eff} in DEMO perspective [6].

2. System description

Starting from the current design of the DTT chamber [7], a first preliminary sketch of a possible liquid metal

author's email: roberto.zanino@polito.it

divertor geometry to fit in the available space has been prepared, see figure 1. This is based on the idea originally proposed by Nagayama [8] and eventually further developed in [9]: the SOL plasma flowing from the main plasma chamber in a reference Single Null (SN) DTT equilibrium enters first the Differential Chamber (DC, see figure 1) and finally the Evaporation Chamber (EC), where the LM pool is located.

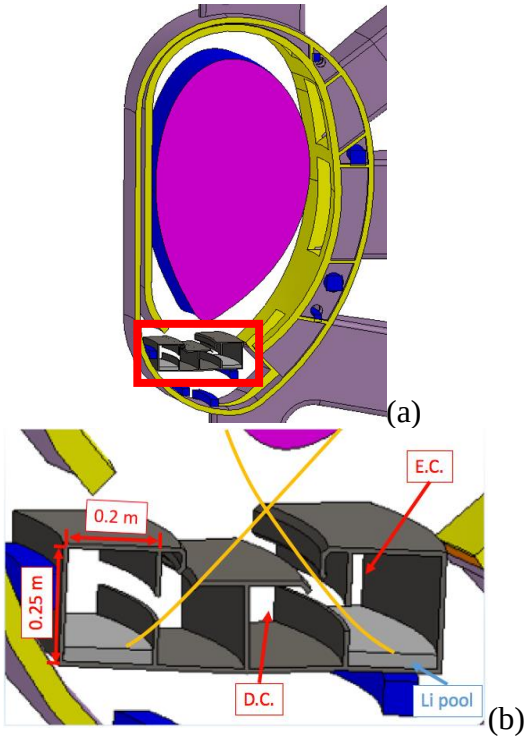

Fig. 1: (a) DTT main plasma chamber with the divertor highlighted and (b) preliminary sketch of the LM divertor.

The schematic representation of the EC used to write down the model equations is shown in figure 2. Even though the shape shown in the schematic is different with respect to the one in figure 1, this is not relevant for a 0D model, the only requirement being to conserve the surface areas and the chamber volumes. The sub-systems are:

- the liquid Li in the pool;
- the Li vapor in the remaining volume of the EC;
- the Li vapor in the DC;
- the solid walls in contact with liquid Li (identified in the following with the subscript *pool*);
- the solid walls in contact with the Li vapor in the EC (identified in the following with subscript *EC*).
- the solid walls in contact with the Li vapor in the DC (identified in the following with subscript *DC*).

3. Phenomenology

The Li evaporating from the pool flows upwards, then either condenses on the relatively colder surfaces of the EC or moves to the DC, where it either condenses or moves outside of the box-structure of the divertor towards the main plasma chamber. The condensed Li is assumed to flow back to the Li pool both from the EC (by gravity) and from the DC (by means of an external circuit, not included in this model for the time being).

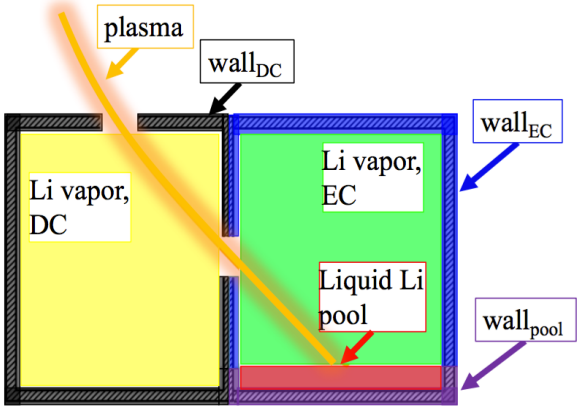

Fig. 2: Schematic of the computational domain.

The presence of a DC in the original Nagayama proposal is motivated by the necessity to reduce the core plasma contamination associated with the eroded (evaporated/sputtered) Li flowing out of the EC. The extra chamber allows for differential pumping, i.e. the connection of two chambers having different pressures by means of intermediate chambers, actively and/or passively pumped (see figure 3). In such a system, when a large pressure difference is involved, choked flow is likely to occur between successive chambers [10].

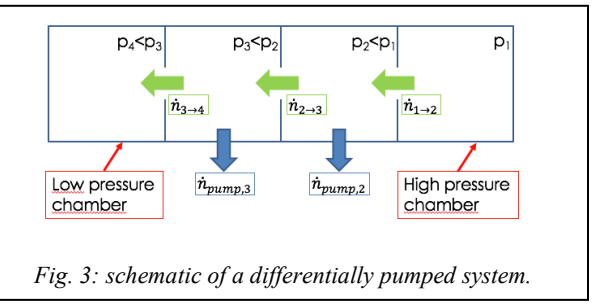

Fig. 3: schematic of a differentially pumped system.

The intermediate chambers allow a progressive reduction in mass flow rate from the higher pressure boxes to the lower pressure boxes, thanks to the – active and/or passive – pumping of the vapor. In the concept considered here, this is achieved by means of net condensation of Li vapor on the walls of the EC and of the DC, i.e. by a passive pumping mechanism. An active differential pumping based on turbomolecular pumps could also be foreseen, in order to differentially pump non-condensable gases.

As it will be pointed out later, the presence of the SOL plasma further reduces the Li efflux between successive chambers (and, eventually, towards the main plasma chamber), thanks to ionization of Li vapor.

Eroded Li is readily ionized by the plasma due to its low first ionization energy (~5 eV), resulting in a significant reduction of the heat flux to the divertor strike point thanks to the related plasma cooling effect [11, 12]. This effect, which in the following will be referred to as the Li "vapor shield", is a consequence of ionization, line

radiation and continuum radiation due to interactions of the free electrons of the SOL plasma with the vapor and could lead to a more manageable flux of Li vapor towards the core plasma (a reduced heat load on the Li pool would reduce the evaporation rate).
From the point of view of the Li mass balance, the fact that Li atoms get "entrained" by the SOL plasma implies a further reduction of the efflux from the EC and consequently from the DC to the main plasma chamber.

The chemical reactivity of liquid Li with hydrogenic species allows in principle the LM to capture fuel particles (increased pumping), allowing a low recycling operation in tokamaks [13], until the Li layer is fully saturated. This occurs because the thermally enhanced diffusion of D atoms in the LM allows in principle to avoid D atoms "piling up" at the surface. Detailed calculations on this point are beyond the scope of this work, but the work in [14] could be employed for a study of D diffusion under various plasma conditions.

An external liquid Li circulation loop for addressing tritium inventory and dust accumulation issues is essential for the steady state behavior of the system hereby analyzed. A detailed analysis of this external loop is beyond the scope of the present work, but recently Ono et al. ([15]) suggested that it is possible to effectively remove tritium and impurities from the liquid Li.

4. Model description

A simplified but self-consistent thermodynamic (0D) model is presented to compute the thermodynamic state of the Li liquid-vapor system, the average wall temperatures and the Li vapor efflux towards the main plasma chamber in an axisymmetric LM divertor of box type. Notwithstanding its simplicity, the model can be considered to be an important step, since a comprehensive analysis of such a system (i.e. a divertor based on the closed-box concept) cannot be found in the literature, to the best of our knowledge, the only pioneering work being the recently published model in [9, 16]. Compared to the latter, the present study employs a transient model in order to reach the steady state, does not assume choked flow between successive boxes and evaluates the average wall temperatures based on the walls energy balance rather than imposing it a priori.
The main assumptions in our model are as follows:

1. The Li vapor is
   a. approximated as an ideal gas. This is verified a posteriori to be acceptable, thanks to the very low pressure foreseen in the EC – see section 5;
   b. monoatomic (the fraction of Li_2 in vapor phase is verified a posteriori to be between 5 and 10% at the temperatures foreseen for this system [17]);
   c. optically thin with respect to radiation, i.e. the radiated power resulting from the interactions between the SOL plasma and the Li vapor is assumed to be deposited on the walls and on the pool surface without absorption within the medium. This is justified due to the extremely low vapor densities expected in the system;
   d. collisional, i.e. the mean free path of the Li atoms in vapor phase is small compared to some characteristic length of the system. Further details concerning this assumption are given in Appendix 1;
   e. partly lost –as a neutral- towards the main plasma chamber and compensated by an equal amount of replenishing liquid Li supplied to the pool, i.e. the total mass of Li in the system is conserved. This simulates the effect of a Li reservoir that is often foreseen in similar systems [18];
   f. partly entrained (ionized) by the plasma and recombining before reaching the pool;
   g. flowing isenthalpically between neighboring boxes;
   h. in thermodynamic equilibrium with the liquid phase.
2. The Li pool
   a. is optically thick with respect to radiation, i.e., it absorbs all radiated power directed towards it, whereas radiation emitted from it to the (colder) walls is negligible with respect to radiation from the Li vapor shield (checked a posteriori);
   b. receives a fraction $f \approx A_{pool}/(A_{w,EC} + A_{pool})$ of the radiated power in the EC, whereas the remaining fraction $(1 - f)$ is directed towards the walls;
   c. instantaneously collects the Li re-condensed on both the EC and DC walls, i.e., the dynamics of the condensed Li film and the external Li recirculation circuit are not included in the model for the time being.
3. The effect of the particle influx from the plasma is neglected, i.e. no account is given here about retention (the properties of the Li pool are not modified), sputtering (no sputtering source has been included in the mass conservation equations for the Li vapor) and pressure build-up due to non-condensable gases (D, T, He).
4. No radiated power is deposited on the DC walls.

The conservation of mass for the Li in the EC (detailed scheme shown in figure 4 and control volume shown in figure 5 (a)) is described by

$$\frac{dN_{Li,EC}}{dt} = \dot{N}_{recollection,EC} + \dot{N}_{repl} + \dot{N}_{recomb,EC} - \dot{N}_{noz,EC\rightarrow DC,noentr} - \dot{N}_{entr,EC} - \dot{N}_{recond,EC} \quad (1)$$

where:

- $N_{Li,EC}$ is the total number of Li atoms in the EC;
- $\dot{N}_{recollection,EC} = \dot{N}_{recond,EC} + \dot{N}_{recond,DC}$ is the particle flow rate of recondensed Li atoms on the walls of both chambers, which are assumed to be instantaneously returned to the pool according to assumption 2c. In particular, $\dot{N}_{recond,EC}$ (atoms/s) is the net re-condensation rate on the walls of the EC,

which is calculated by means of a modified Hertz-Knudsen equation [19]

$$\dot{N}_{recond,EC} = \dot{N}_{cond,EC} - \dot{N}_{ev,EC} = \eta \cdot A_{w,EC} \cdot 10^3 \cdot \left(\frac{p_{EC} \cdot N_{Av}}{\sqrt{2\pi m_{Li} R_0 T_{EC}}} - \frac{p_{sat}(T_{EC}) \cdot N_{Av}}{\sqrt{2\pi m_{Li} R_0 T_{w,EC}}}\right) \quad (2)$$

where $\dot{N}_{cond,EC}$ (atoms/s) is the condensation rate to the walls of the EC, $\dot{N}_{ev,EC}$ (atoms/s) is the evaporation rate from the EC, T $T_{w,EC}$ (K) is the temperature of the EC walls, T_{EC} (K) is the temperature of the Li vapor in the EC, $p_{sat}(T_{EC})$ (Pa) is the saturation pressure evaluated at T_{EC}, p_{EC} (Pa) is the pressure of Li vapor. η is an empirical coefficient estimated in [19] to be equal to 1.66, $A_{w,EC}$ (m^2) is the surface area of the EC walls facing the Li vapor, m_{Li} (g/mol) is the molar mass of Li, N_{Av} is the Avogadro number and R_0 (J/kmol/K) is the universal gas constant. (A more detailed analysis including an energy balance for the Li film would be more appropriate, but this is left for future work). The same approach is employed for evaluating $\dot{N}_{recond,DC}$..

- $\dot{N}_{recomb,EC} = \dot{N}_{entr,EC} + \dot{N}_{entr,EC\to DC} + \dot{N}_{entr,DC} + \dot{N}_{entr,DC\to MC}$ is the particle flow rate of Li atoms entrained by the plasma in the entire system, which are all assumed to recombine within the EC. Indeed, as recombination is assumed to occur in the EC, from the Li particle balance point of view, it means that also atoms ionized in the DC enter the particle balance within the EC as a source term. In particular, $\dot{N}_{entr,EC}$ (atoms/s) is the particle flow rate of Li vapor entrained by the plasma within the EC, evaluated relying on the statistical mechanics formulation of the particle flux striking on a surface (Langmuir flux), which assumes a Maxwellian distribution of the atoms. The nature of this expression is therefore exactly the same as the original Hertz-Knudsen one (i.e. equation (2) without the η factor), but for a "purely condensing wall" [10], since the plasma cannot release entrained atoms until recombination has occurred: *locally*, it acts as a perfect particle sink. The area employed in this formulation is the outer surface of the SOL plasma in the EC. $\dot{N}_{entr,DC}$ is evaluated in the same way.
.
- $\dot{N}_{entr,EC\to DC}$ (atoms/s) is the particle flow rate of Li vapor entrained by the plasma while passing from EC to DC, evaluated as:

$$\dot{N}_{entr,EC\to DC} = \dot{N}_{noz,EC\to DC,noentr} \cdot \left(\frac{\lambda_{p,OMP}}{A_{noz}} \cdot f_{EXP}\right) \quad (3)$$

where $\dot{N}_{noz,EC\to DC,noentr}$ (atoms/s) is the Li vapor flow rate from the EC to the DC through the aperture (nozzle) between the two, evaluated assuming isenthalpic flow and neglecting the presence of the plasma:

$$\dot{N}_{noz,EC\to DC,noentr} = \left[\rho_{noz} \cdot A_{noz} \cdot \sqrt{2 \cdot \frac{\gamma}{\gamma-1} \cdot \left(\frac{p_{EC}}{\rho_{EC}} - \frac{p_{noz}}{\rho_{noz}}\right)}\right] \cdot \frac{N_{Av}}{m_{Li}} \cdot 10^3 \quad (4)$$

where ρ (kg/m^3) is a density, A_{noz} (m^2) is the passage area between boxes, γ = 5/3 is the isentropic exponent and the subscript *noz* refers to gas conditions at the nozzle. In particular:

- if $\frac{p_{DC}}{p_{EC}} \le \left(\frac{2}{\gamma+1}\right)^{\frac{\gamma}{\gamma-1}}$, then $p_{noz} = p_{EC}\left(\frac{2}{\gamma+1}\right)^{\frac{\gamma}{\gamma-1}}$ -- the so called *choked flow* condition;
- if $\frac{p_{DC}}{p_{EC}} > \left(\frac{2}{\gamma+1}\right)^{\frac{\gamma}{\gamma-1}}$, then $p_{noz} = p_{DC}$ -- the subcritical flow condition.

- $\lambda_{p,OMP}$ is the power scrape-off width evaluated by means of the model in [20], whereas the term $f_{EXP} = \frac{(B_\theta/B_\phi)_{OMP}}{(B_\theta/B_\phi)_{noz,EC\to DC}}$ takes into account the flux expansion from the outboard midplane to the location of the aperture [21].
- $\dot{N}_{entr,DC\to MC}$ is the particle flow rate of Li vapor entrained by the plasma while passing from DC to MC, and is evaluated in the same way as $\dot{N}_{entr,EC\to DC}$.
- $\dot{N}_{noz,EC\to DC}$ (atoms/s) is the Li vapor flow rate from the EC to the DC through the nozzle, evaluated by subtracting $\dot{N}_{entr,EC\to DC}$ from $\dot{N}_{noz,EC\to DC,noentr}$.
- $\dot{N}_{repl}$ (atoms/s) is the rate of liquid Li replenishment to the pool in order to compensate for the loss of Li vapor towards the main plasma chamber:

$$\dot{N}_{repl} = \dot{N}_{noz,DC\to MC} \quad (5)$$

where the latter quantity is evaluated in the same way as $\dot{N}_{noz,EC\to DC}$.

The conservation of energy for the Li in the EC (control volume shown in figure 5 (a)) is described by

$$\frac{d(U_{Li,EC} - U_0)}{dt} = \left((G \cdot h)_{ev,w} - (G \cdot h)_{cond,w}\right)_{EC} + (G \cdot h)_{entr,DC} + (G \cdot h)_{entr,DC\to MC} - (G \cdot h)_{noz,EC\to DC} + f \cdot \Phi_{rad} + \Phi_{plasma\to pool} - \Phi_{pool\to w} \quad (7)$$

where $U_{Li,EC}$ (J) is the total internal energy of the Li system, whereas U_0 is the internal energy of the system in the reference conditions.

Evaluation of the thermodynamic quality in the EC is performed by means of the usual thermodynamic relations for two-phase systems in equilibrium conditions:

$$\left(U_{Li,EC} - U_0\right) = (1-x) \cdot M_{Li,EC} \cdot u_f(T_{sat}) + x \cdot M_{Li,EC} \cdot u_g(T_{sat}) \quad (8)$$

$$\frac{V_{EC}}{M_{Li,EC}} = (1-x) \cdot v_f(T_{sat}) + x \cdot v_g(T_{sat}) \quad (9)$$

where V_{EC} (m^3), volume of the EC, is constant, whereas $M_{Li,EC}$ (kg), total mass of Li inside the EC, is evaluated by means of (1). It is possible to iteratively solve this system of two equations in two unknowns in order to find values of x and of the (T_{sat}, p_{sat}) pair at each time step.

The $(G \cdot h)$ terms in eq. (7) represent the heat fluxes associated with mass fluxes, evaluated as the product of the mass flow rates in kg/s and the suitable specific enthalpies in J/kg. In particular, the terms indicated by *ev* and *cond* correspond to the two contributions to $\dot{N}_{recond,DC}$ indicated in eq. (2). $h_{cond,w,EC}, h_{ev,w,EC}, h_{entr,EC}, h_{noz,EC\to DC}$ are the specific enthalpies carried by $G_{cond,w,EC}$, $G_{ev,w,EC}$, $G_{entr,EC}, G_{noz,EC\to DC}$, respectively. The value of all these enthalpies is equal to $h_v(T_{EC}, p_{EC})$, i.e. the enthalpy of Li vapor in the EC. It should be noticed that, since the total enthalpy is conserved in the efflux from the EC to the DC, and the Li vapor in the DC is stationary, the term $h_{noz,EC\to DC}$ is found unchanged also in the energy balance of the DC, see below.

$\Phi_{plasma\to pool}$ (W) is the amount of the incoming plasma heat load which is not radiated, evaluated as

$$\Phi_{plasma\to pool} = \Phi_{SOL} - \Phi_{rad} \qquad (10)$$

where Φ_{SOL} is the incoming heat load associated with the plasma and Φ_{rad} is the amount of power radiated in consequence of the above described Li "vapor shield" effect. A simplified approach for quantifying the latter is hereby proposed, based on [9, 12]. The amount of the incoming heat load associated with the plasma which is lost due to interactions with the Li vapor shield, is evaluated as follows:

$$\Phi_{cool} = \varepsilon_{cool} \cdot e \cdot \left(\dot{N}_{entr,EC} + \dot{N}_{entr,EC\to DC} + \dot{N}_{entr,DC} + \dot{N}_{entr,DC\to MC}\right) \qquad (11)$$

where ε_{cool} (eV) represents the cooling energy per Li atom, e is the conversion factor from J to eV.

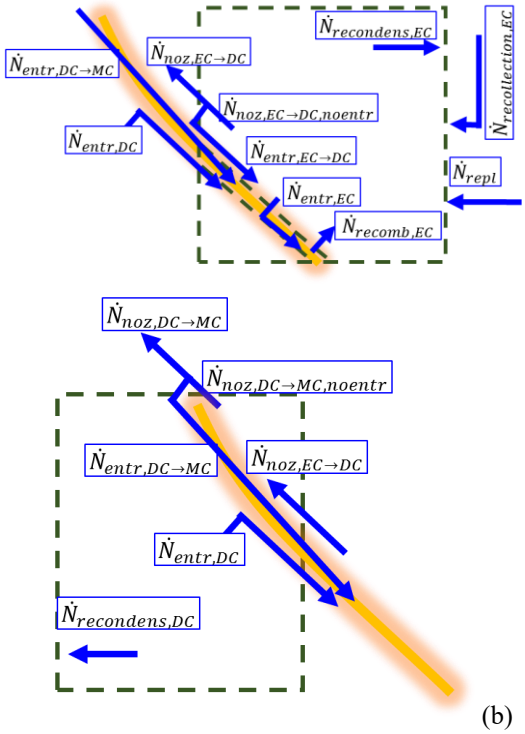

Fig. 4:Detail of the particle balance within EC (a) and DC (b).

This expression states that each atom interacting with the plasma removes ε_{cool} eV from the plasma. Goldston [9] has recently obtained a model for quantitatively assessing the functional dependence of ε_{cool} on the SOL plasma temperature and density. Based on these results applied to the system under study, it can be stated that a conservative value for the ε_{cool} is roughly 10 eV.
In this study, the following assumptions are made:

1. recombination occurs in the EC;
2. radiation is negligible in the DC.

Based on these assumptions, it is possible to approximate as follows:

$$\Phi_{rad} \approx \Phi_{rad,EC} \approx \Phi_{cool} \qquad (12)$$

This power, radiated in the EC, is partly directed towards the pool surface and partly directed towards the walls, and it is assumed to be completely absorbed by walls/pool surface.

$\Phi_{pool\to w}$ (W) is the power transferred from the liquid Li in the pool to the part of the wall in contact with it. In this simplified model, the heat conduction between the wall fraction in contact with the liquid phase and the one in contact with the vapor phase is neglected. It is also assumed that the heat capacity of the fraction of the wall in contact with liquid Li is negligible. Hence

$$\Phi_{pool\to w} = \Phi_{active\ cooling,w,pool} \qquad (13)$$

where $\Phi_{active\ cooling,w,pool} = H \cdot A_{w,pool} \cdot \left(T_{w,pool} - T_{coolant}\right)$ where H ($W/m^2/K$) is the global heat transfer coefficient between the wall and the cooling water,

accounting for both conductive and convective thermal resistances, $A_{w,pool}$ (m^2) is the interface area and $T_{coolant}$ (K) is the temperature of the coolant.

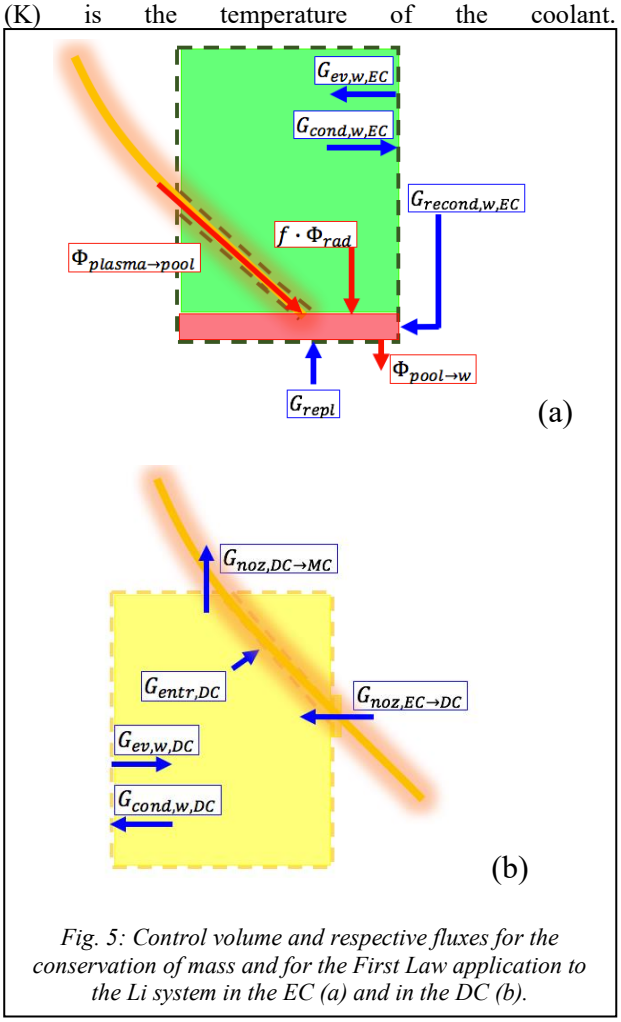

Fig. 5: Control volume and respective fluxes for the conservation of mass and for the First Law application to the Li system in the EC (a) and in the DC (b).

The conservation of mass for the Li vapor in the DC (control volume shown in figure 5 (b)) is described by

$$\frac{dN_{Li,DC}}{dt} = -\dot{N}_{recond,DC} - \dot{N}_{entr,DC} + \dot{N}_{noz,EC \to DC} - \dot{N}_{noz,DC \to MC} \quad (14)$$

where the meaning of the remaining symbols is clear from the previous discussion.

The conservation of energy for the vapor in the DC (control volume shown in figure 5 (b)) is described by

$$\frac{d(U_{Li,DC} - U_0)}{dt} = \left((G \cdot h)_{ev,w} - (G \cdot h)_{cond,w}\right)_{DC} - (G \cdot h)_{entr,DC} + (G \cdot h)_{noz,EC \to DC} - (G \cdot h)_{noz,DC \to MC} \quad (15)$$

Where all the terms of specific enthalpy of the Li vapor in the DC are suitably evaluated at T_{DC} and p_{DC}.

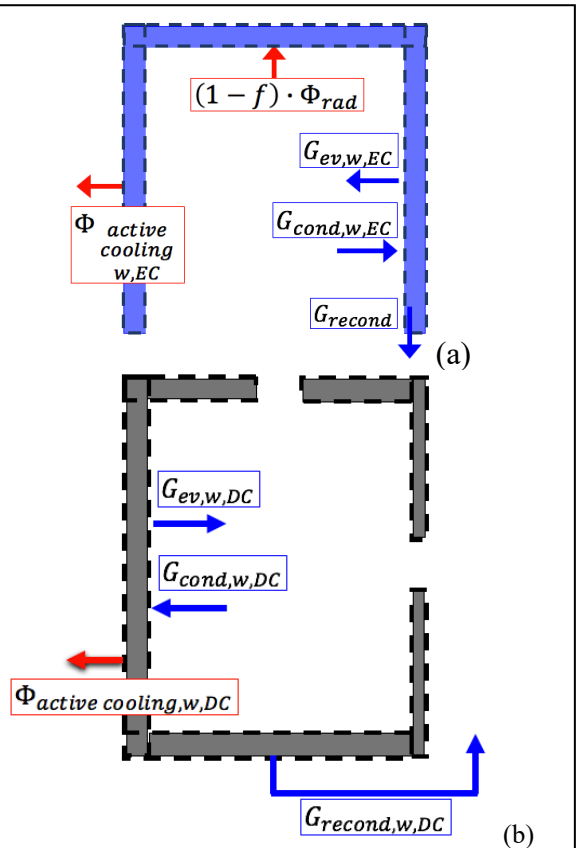

Fig. 6: Control volume for conservation of energy for the walls of the EC (a) and DC (b)

The conservation of energy for the walls in contact with the Li vapour in the EC (control volume shown in figure 6 (a)) is described by

$$V_{w,EC}(\rho c)_{w,EC}\frac{dT_{w,EC}}{dt} = = (1-f) \cdot \Phi_{rad} + \left((G \cdot h)_{cond,w} - (G \cdot h)_{ev,w}\right)_{EC} - \Phi_{active\ cooling,w,EC} \quad (16)$$

where $V_{w,EC}$ (m^3) is the volume of wall$_{EC}$, $\rho_{w,EC}$ (kg/m^3) is the density of the material used for the walls, $c_{w,EC}$ (J/kg/K) is the specific heat of the material used for the walls, $\Phi_{active\ cooling,w,EC}$ (W) is the power removed from the walls of the EC not in contact with the Li pool by means of active cooling, which can be preliminary estimated as

$$\Phi_{active\ cooling,w,EC} = H \cdot A_{w,EC} \cdot \left(T_{w,EC} - T_{water}\right) \quad (17)$$

where $A_{w,EC}$ (m^2) is the interface area.
Since this expression describes the energy balance of the walls, it may be surprising to find here heat fluxes associated with mass fluxes. This is actually due to the fact that the wall and the Li re-condensing film (or the wall and the liquid Li-carrying wick in case the walls are coated by a CPS) are considered within the same control volume, as a model for the re-condensing Li film has not yet been developed by our group. In this open system, mass exchanges are allowed by evaporation, condensation and, in the end, recollection of the liquid Li to be redirected to the pool, whereas heat fluxes are present due to radiation (in the EC) and active cooling.

The conservation of energy for the walls in contact with the Li vapour in the DC (control volume shown in figure 6 (b)) is described by

$$V_{w,DC}(\rho c)_{w,DC}\frac{dT_{w,DC}}{dt} = \left((G\cdot h)_{cond,w} - (G\cdot h)_{ev,w}\right)_{DC} - \Phi_{active\ cooling,DC} \qquad (18)$$

5. Application of the model to a reference DTT scenario

The set of coupled, nonlinear ODEs (1), (7), (14), (15), (16), (18) presented above has been solved by means of an explicit Runge-Kutta method of order four with adaptive timestep (routine ode113 in Matlab®) and input data as specified in Table 1.

Table I: Input data for the reference scenario

Quantity	Value	Source
Φ_{SOL}	32 MW	[6]
A_{pool}	4.56 m^2	CAD
$A_{w,EC}$	15.9 m^2	CAD
f	0.169	CAD
$T_{coolant}$	200 °C	[5]
H	5000 W/m^2 K	[24]
ε_{cool}	100 eV	[22]
w_{noz}	5 cm	CAD

Only the outboard divertor is studied, with an inlet heat load of 21 MW/m^2 (i.e. 2/3 of the total power crossing the separatrix), according to conservative DTT specifications [6]. It should be noticed that in a 0D model as the present one this corresponds to a flux of ~9 MW/m^2 on the pool surface if no vapour shielding was present, whereas the estimated peak heat flux from 2D plasma analysis in DTT, in the absence of divertor radiation, is ~ 54 MW/m^2 [6]. This implies that this model is not able to evaluate the peak temperature in the divertor.

The walls are assumed to be made of stainless steel, and their thermophysical properties are consequently evaluated. The properties of liquid Li are evaluated according to [23] and the properties of stainless steel are assumed to be independent on temperature and evaluated from [24].

5.1. Transient behaviour of the system

The transient calculation starts from an equilibrium situation in which the walls and the liquid Li in the pool are at $T_{coolant}$ (see table 1) and the vapor in the two chambers is in saturation conditions at that temperature.

At time t = 0+ the heat load associated with the plasma is turned on. At the beginning, this heat load is almost entirely directed towards the pool, since the effect of the lithium vapor shield is small, due to the small quantity of entrained Li, see eq. (11). This drives an initial steep temperature increase of the Li system and of the thermodynamic quality. The larger density of vapor in the two chambers causes the radiated fraction of the incoming heat load to increase. At this point the heat load to the pool has been reduced and the Li temperature reaches a steady state value determined by the balance between this power and the active cooling power. The temperature evolution is shown in figure 7, where $T_{EC} = T_{pool} = T_{vap,EC}$.

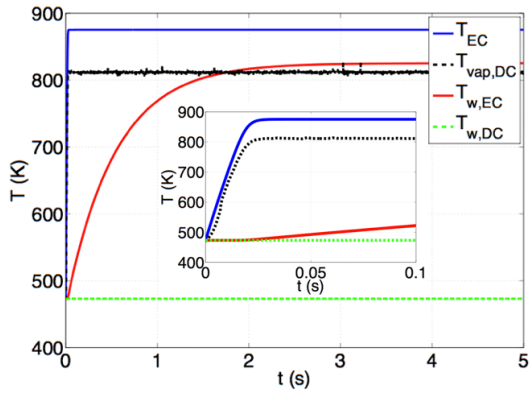

Fig. 7: Evolution of the temperatures of the subsystems for the reference scenario (inset: first part of the transient).

5.2. Influence of the cooling energy per Li atom (ε_{cool})

Since, as explained above, ε_{cool} is subject to large uncertainties, a first parametric study has been performed on this quantity, whose results are shown in figure 8, varying it from 10 eV up to 250 eV. As this parameter is increased, the incoming heat load associated with the plasma is increasingly spread over the EC walls instead of being only directed towards the Li pool (this can be seen from the decrease of $\Phi_{pool\to w}$ and the corresponding increase of $\Phi_{active\ cooling,w,EC}$ shown in figure 8 (a). This implies a lower temperature of the liquid-vapor system (and therefore a lower vapor density, following the assumption of thermodynamic equilibrium between the phases) and a higher wall temperature (figure 8 (b)). Figure 8 (b) shows that the value of ε_{cool} mainly influences the pressure (blue, solid line) of the Li liquid-vapor system in the EC, whereas the operating temperature of the LM coating (magenta, dashed line) is quite insensitive to this parameter, as a consequence of the correlation between temperature and pressure in saturation conditions.

This implies that, if the Li vapor shield is taken into account, the plasma heat load is exhausted without a large

increase of the Li pressure in vapor phase with respect to the initial condition, i.e. with a lower mass flow rate towards the main plasma chamber, as shown in figure 9.

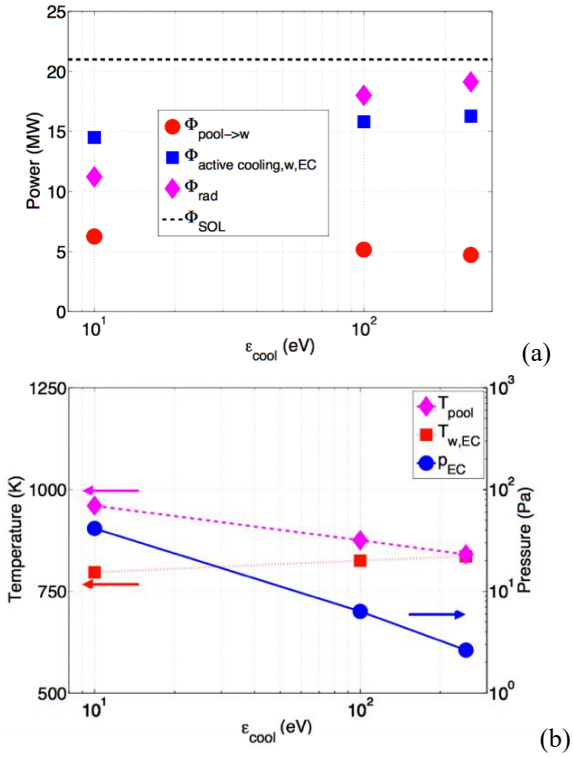

Fig. 8: Parametric study of the effects of ε_{cool} on $\Phi_{pool\rightarrow w}$, $\Phi_{active\ cooling,w,EC}$, Φ_{rad} (respectively defined in equation (13), (16), (4) (a), on liquid and wall temperatures (red, left axis) and pressure (blue, right axis) (b).

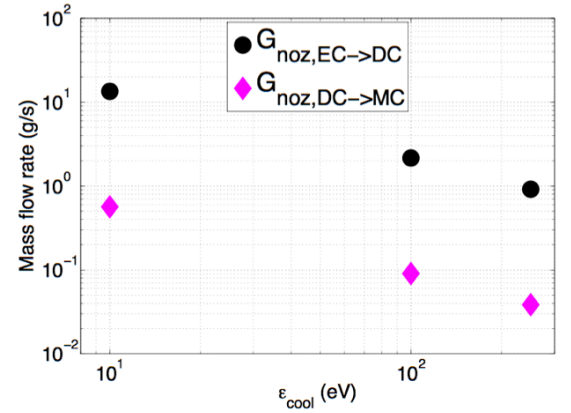

Fig. 9: Effect of the radiated energy per Li atom on the Li vapor mass flow rates

This parametric study also provides a first idea of the range of parameters to be expected in such a system, which is useful in order to a posteriori verify some of the assumptions. For instance, neglecting the sputtered Li flux from the liquid/vapor interface is justified by the fact that, for all the values of ε_{cool} considered, the pool temperature is larger than 500°C [14]. Moreover, the temperatures of the pool are generally larger than the decomposition temperature of LiD (and LiT), see [25]. This means that the full D retention observed for liquid Li coatings, which would allow the tokamak to operate in a low recycling regime, may not occur. Since the latter represents the main motivation for using Li instead of other LMs as divertor coating, this consideration may re-open the discussion concerning other LMs. Sn, for instance, [26] would not allow low recycling operation but has a much larger latent heat of evaporation which could compensate for its larger core plasma contamination. Moreover, the effects of this reduced T retention at high temperatures on the strategies for tritium removal would require further studies. Finally, densities foreseen in the EC in the reference scenario are of the order of 10^{21} atoms/m^3. With such values, based on a simplified model for estimating the plasma parameters proposed in [27] (not shown here) plasma is expected to radiate most of its energy within the EC. Therefore, assuming that recombination occurs before reaching the surface appears to be acceptable.

It is interesting to point out that increasing ε_{cool} implies a reduction of the thermodynamic quality in the EC, since less Li is evaporated (see figure 10). The value of the quality is low in all cases due to the initial quantity of liquid Li assumed for the calculations.

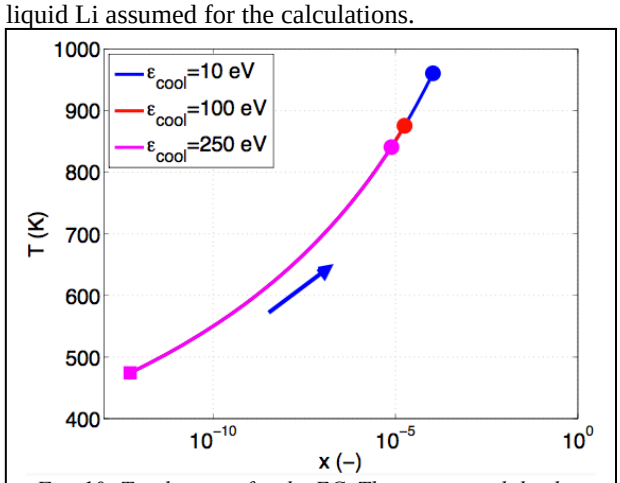

Fig. 10: T-x diagram for the EC. The square and the dots indicate the starting point and the final point of the trajectories, respectively.

The dependence of the thermodynamic state of the EC on ε_{cool} has been assessed also for the case H = 500 W/(m^{2}K), see figure 11. The fact that this thermodynamic state is independent of ε_{cool} is not surprising, since this low value of the heat transfer coefficient implies hotter walls, lower condensation and therefore a larger thermodynamic quality and pressure with respect to large values of the heat transfer coefficient. The density in the EC determines the probability that a Li atom is entrained and thereby radiates the corresponding ε_{cool}, and this phenomenon is subject to a saturation since, obviously, the radiated power can at most be equal to Φ_{SOL}. For large values of the density, the entire Φ_{SOL} is radiated even with low values of ε_{cool} , since more Li atoms interact with the plasma.

5.3. Influence of nozzle aperture

It is important to assess the influence of the width of the aperture between successive chambers (the apertures between EC and DC and between DC and MC are hereby assumed to be equal) on the thermodynamic state of the system and, even if only qualitatively, on the Li vapor

efflux towards the MC, since large design tolerances are foreseen concerning this parameter. indeed, it is through

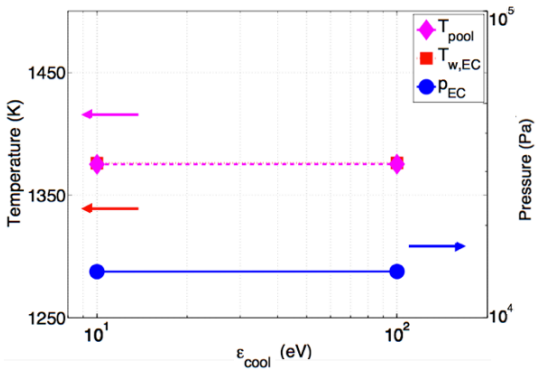

Fig. 11: Thermodynamic state of the Li system as a function of ε_{cool} for H=500 W/(m²K).

these "nozzles" that the plasma flux around the separatrix is directed towards the pool and too tight tolerances (i.e., a too narrow aperture), could easily lead to intolerable plasma heat load and sputtering around the aperture, in case of a plasma displacement.

Here we conservatively consider that the aperture width should be at least three times larger than the power scrape-off width. The latter is estimated to be ~ 2.1 mm at the DTT outboard midplane based on [19], and considering flux expansion it could easily reach ~ 1 cm at the DC entrance. This would place a lower bound to the aperture width of 3 cm. It is to be noticed, however, that the *density* scrape-off width is larger than the power scrape-off width. It appears therefore that a conservative estimate for the aperture width is 5 cm, which is the value indicated in table 1. During startup or during plasma instabilities, however, the position of the separatrix will vary, and this should be taken into account in order to avoid the aforementioned problems.

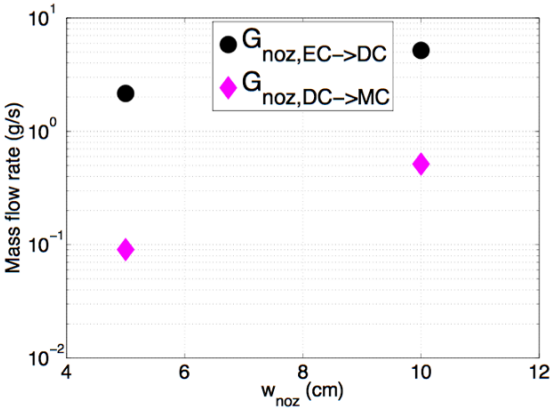

Fig. 12: Effect of the nozzle aperture on the Li vapor mass flow rate.

A case having an aperture width of 10 cm is therefore also analysed, with results shown in figure 12. Although the actual limit on the allowable Li vapor flow rate has to be found by means of more accurate plasma modelling, it can be stated that the presence of the DC alone allows reducing the Li mass flow rate towards the main plasma chamber by a factor ~10. In order to further reduce the Li outflow from the divertor, one could add an additional differential chamber, if enough space is available.

5.4. Influence of *f* (fraction of the radiated power in the EC absorbed by the pool)

The value $f = 0.169$ reported in Table 1 has been used for the parametric studies presented so far, but the actual value of this parameter depends on the actual radiation distribution within the EC, which can only be determined by means of 2D plasma codes (e. g. SOLPS).

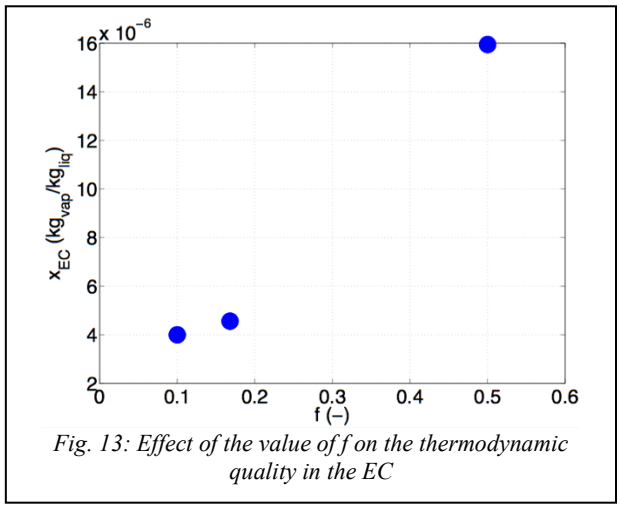

Fig. 13: Effect of the value of f on the thermodynamic quality in the EC

Therefore, a case with $f = 0.5$ has been considered as an upper bound (since this corresponds to the case of a "radiative layer" formed upon the pool radiating half of its power towards the latter). A lower bound of 0.1 has been included, corresponding to radiation taking place at the entrance of the EC. Figure 13 shows the dependence of the thermodynamic quality of the Li vapor system in the EC on the parameter *f*. As expected, the quality increases as f increases since this implies a larger amount of radiated power directed towards the pool, increasing the internal energy of the Li system.

6. Conclusions and future developments

A first study of a possible liquid metal divertor for the Divertor Tokamak Test (DTT) has been presented.

Starting from the preliminary CAD of the DTT internal components, a preliminary dimensioning of the system has been proposed.

A thermodynamic (0D) model of the system has been developed including a simplified treatment of the interactions of the Li vapor with the SOL plasma. The model shows that the expected temperatures of the Li system are of the order of 900-1000 K. This is a rough yet important information for the choice of the wall materials, which must be done according to the compatibility with hot Li, and to assess the recycling coefficient expected at the wall.

It is recognized that fluid modeling as adopted here is only adequate in the EC, whereas for an accurate description of the Li vapor in the second chamber, which would allow quantitative estimations on the Li efflux towards the main

plasma, methods such as DSMC ([28]) should be employed.
Although the used 0D approach does not allow for hot spot temperature estimations, it can be stated that the effect of Li in terms of heat flux redistribution from the target to the EC walls is effective, thanks in particular to the Li vapor shield effect.
Finally, since the pool temperature exceeds the decomposition temperature of LiD [25], it appears that a high recycling regime is more probable in such device. In order to benefit from the low recycling regime which has often motivated the choice of Li with respect to other metals such as Sn, a particular cooling strategy should be foreseen.
Thanks to the modularity of the 0D model proposed, which allows to easily implement different LM choices, future work will investigate the possible effects of using Sn instead of Li as LM for the target, or, possibly, Li-Sn alloys. More detailed simulations should be performed, including 2D modeling of both the plasma species and of the neutrals, for instance by means of the SOLPS suite. It must be remarked that the treatment of ionized Li has been extremely simplified throughout this work. Detailed treatment of ionization, line radiation/bremsstrahlung and recombination should provide a detailed description of the radiated power source which dominates the energy balance in this system.
An important missing piece of the model is the presence of noncondensable gases. In particular, the possibility of passively pumping He, D and T should be carefully assessed, since this would constitute a key advantage of this system.
It is also clear that the simple pool option hereby presented would be subject to MHD instabilities. A detailed analysis of a CPS-based liquid metal divertor, which arguably is the most promising choice in terms of LM stability and robustness, should therefore be performed, but the thermodynamic basis is the same. This would place an additional limit on the operating space. Moreover, the closed-box divertor approach allows to easily confine the Li vapor but has some geometrical incompatibilities. A different, entirely CPS-based solution like the one proposed in [4], could be studied in the future.

Appendix 1: Considerations on the Knudsen number

Many of the correlations employed -including the formula for efflux of a compressible gas through an aperture, the expressions for evaporation and condensation fluxes and for the particle flow rate of entrained Li- rely on the collisionality of the Li vapor. It is well known that for this to apply it is necessary that the mean free path of the particles is small compared to a characteristic length of the system. This is quantified by the Knudsen number. The latter is defined as [28]

$$Kn = \frac{\lambda}{L} \qquad (19)$$

where λ is the mean free path of the particle and L is the characteristic length of the gradients in the Li flow. In particular, for a Boltzmann gas the mean free path can be evaluated as [29]

$$\lambda = \frac{k_b \cdot T}{\sqrt{2} \cdot \pi \cdot d^2 \cdot p} \qquad (20)$$

where d is the Van der Waals diameter of the particle (for Li atoms: d = 182 pm).
In a detailed simulation, where differential mass, momentum and energy balances are solved, it is possible to evaluate a *local* Knudsen number using as length the scale length of macroscopic gradients of the flow (for example, using the density, $L \approx \rho/\nabla\rho$). In the present 0D model this is not possible and therefore L must be assumed to be equal to some macroscopic length of the system.
Based on the typical classification of the flow regimes, the value $Kn \sim 0.1$ (red dashed line in figure 14) can be taken as an upper bound for the applicability of continuum models to the study of the behavior of the Li vapor in this system.

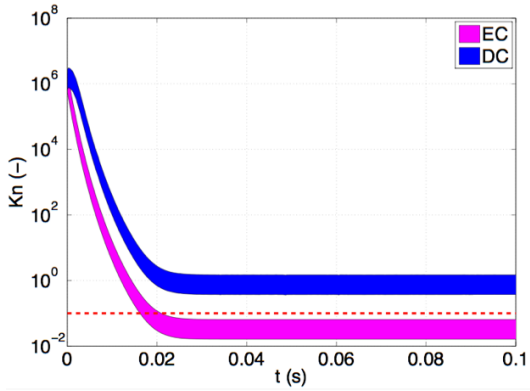

Fig. 14: evolution of the Knudsen number in the two chambers.

This is an important information in terms of the choice of the suitable tool for future studies and in terms of the relevance of the initial transient results. Indeed figure 14 shows the values of the Knudsen number for the EC and the DC, where both the aperture/transverse size of the nozzles (L=0.05 m) -upper bound- and the box width (L=0.2 m) -lower bound- are used as characteristic length in the definition of *Kn*, thereby obtaining a range where the actual, local *Kn* is expected to be found [10]. The pressure and temperature employed in (20) correspond to thermodynamic conditions within the boxes.
The dependence of the Knudsen number on the value of ε_{cool} has also been assessed, see figure 15.

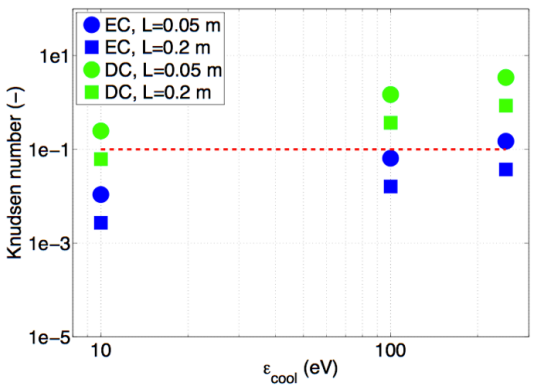

Fig. 15: Knudsen number evaluation at various locations for H=5000 W/m²K. The red dotted line indicates the typical applicability limit for continuum models.

The plot shows that reducing ε_{cool}, i.e. progressively "switching off" the Li vapor shield effect, yields a reduction in the Knudsen number.

This is due to the fact that, if the radiated power decreases, the heating of the pool is stronger and therefore a larger quantity of Li vaporizes (larger thermodynamic quality, see figure 10), notwithstanding the increase of the temperature of the walls.
In the parameter space explored in this study the value of *Kn* for the DC is always $\gtrsim 0.1$. It should therefore be kept in mind that conclusions concerning the DC, including the actual Li vapor flow from the DC to the MC, are to be considered as purely qualitative.

Acknowledgments

The authors would like to thank Giuseppe di Gironimo for the DTT CAD, Rob Goldston and the members of the CIRTEN Consortium for several discussions.

References

[1] EFDA, Fusion Electricity: A roadmap to the realisation of fusion energy, 2012, ISBN 978-3-00-040720-8, available online at https://www.euro-fusion.org/wpcms/wp-content/uploads/2013/01/JG12.356-web.pdf.

[2] R. Zagorski, V. Pericoli, H. Reimerdes, R. Ambrosino, H. Bufferand, G. Calabro et al., Evaluation of the power and particle exhaust performance of various alternative divertor concepts for DEMO, EUROFUSION WPDTT1-PR (2016) 16271, available online at http://www.euro-fusionscipub.org/wp-content/uploads/WPDTT1PR16_16271_submitted.pdf.

[3] M. Merola, F. Escourbiac, R. Raffray, P. Chappuis, T. Hirai and A. Martin, Overview and status of ITER internal components, Fusion Engineering and Design 89 (2014), 890–895.

[4] L. G. Golubchikov, V. A. Evtikhin, I. E. Lyublinski, V. I. Pistunovich, I. N. Potapov and A. N. Chumanov, Development of a liquid-metal fusion reactor divertor with a capillary-pore system, Journal of Nuclear Materials 233-237 (1996) 667-672.

[5] G. Mazzitelli, M. L. Apicella, A. Alexeyev and the FTU team, Heat loads on FTU liquid lithium limiter, Fusion Engineering and Design 86 (2011), 580–583.

[6] R. Albanese, DTT: a divertor tokamak test facility for the study of the power exhaust issues in view of DEMO, Nuclear Fusion 57 (2016) 016010.

[7] G. Di Gironimo, private communication, Jun 2016.

[8] Y. Nagayama, Liquid lithium divertor system for fusion reactor, Fusion Engineering and Design 84 (2009) 1380-1383.

[9] R. Goldston, R. Myers and J. Schwartz, The lithium vapor box divertor, Physica Scripta T167 (2016) 014017 (6pp).

[10] H. J. N. Van Eck, W. R. Koppers, G. J. van Rooij, W. J. Goedheer, R. Engeln, D. C. Schram, N. J. Lopes Cardozo and A. W. Kleyn, Modeling and experiments on differential pumping in linear plasma generators operating at high gas flows, Journal of Applied Physics 105 (2009), 063307 (11 pp.).

[11] G. Mazzitelli, Liquid metal: feedback from FTU, 22nd Int. Conference on Plasma Surface Interaction in Controlled Fusion Devices (oral presentation), Rome (2016), available online.

[12] R. E. Nygren and F. L. Tabarés, Liquid surfaces for fusion plasma facing components—A critical review. Part I: Physics and PSI, Nuclear Materials and Energy 9 (2016) 6–21.

[13] R. Majeski, R.E. Bell, D.P. Boyle, R. Kaita, T. Kozub, B.P. LeBlanc, M. Lucia, R. Maingi, E. Merino, Y. Raitses, J.C. Schmitt, J.P. Allain, F. Bedoya, J. Bialek, T.M. Biewer, J.M. Canik, L. Buzi, B.E. Koel, M.I. Patino, A.M. Capece, C. Hanses, T. Jarboe, S. Kubota, W.A. Peebles and K. Tritz, Compatibility of lithium plasma-facing surfaces with high edge temperatures in the Lithium Tokamak Esperiment, Physics of Plasmas 24 (2017) 056110.

[14] T. Abrams, M. Jaworski, Suppressed gross erosion of high-temperature lithium via rapid deuterium implantation, Nuclear Fusion 56 (2016) 016022 (10pp).

[15] M. Ono, M. A. Jaworski, R. Kaita, Y. Hirooka, T. K. Gray and the NSTX-U Research Team, Liquid lithium applications for solving challenging fusion reactor issues and NSTX-U contributions, Fusion Engineering and Design 117 (2017) 124–129.

[16] R. Myers, A Lithium Vapor-Box Divertor for Tokamak Applications (MSc thesis), Princeton University (2015).

[17] P. Pascal, Nouveau traité de Chimie Minérale, Masson, Paris, 1966.

[18] S. Mirnov, A. M. Belov, N. T. Djigailo, A. S. Dzhurik, S. I. Kravchuk, V. B. Lazarev, I. E. Lyublinski, A. V. Vertkov, M. Yu. Zharkov and A. N. Shcherbak, Experimental test of the system of vertical and longitudinal lithium limiters on T-11M tokamak as a prototype of plasma facing components of a steady-state fusion neutron source, Nuclear Fusion 55 (2015) 123015 (11pp).

[19] J. Safarian, T. A. Engh, Vacuum Evaporation of Pure Metals, Metallurgical and Materials Transactions A, 44 (2013) 747-753.

[20] R. Goldston, Heuristic drift-based model of the power scrape-off width in low-gas-puff H-mode tokamaks, Nuclear Fusion 52 (2012) 013009 (7pp).

[21] V. A. Soukhanovskii, R.E. Bell, A. Diallo, S. Gerhardt, S. Kaye, E. Kolemen et al., Advanced divertor configurations with large flux expansions, Journal of Nuclear Materials 438 (2013), p. S96-S101.

[22] R. Goldston, A. Hakim, G.W. Hammett, M.A. Jaworski, J. Schwartz, Recent advances towards a lithium vapor box divertor, Nuclear Materials and Energy (in press), https://doi.org/10.1016/j.nme.2017.03.020.

[23] International Atomic Energy Agency, Thermophysical Properties of Materials for Nuclear

Engineering: A Tutorial and Collection of Data, IAEA, Vienna (2008).
[24] T. L. Bergman, A. S. Lavine, F. P. Incropera and D. P. Dewitt, Introduction to Heat Transfer, Wiley, 2011.
[25] M. J. Baldwin, R.P. Doerner, S.C. Luckhardt and R.W. Conn, Deuterium retention in liquid lithium, Nuclear Fusion 42 (2002) 1318–1323.
[26] R. Majeski, Liquid Metal Walls, Lithium, And Low Recycling Boundary Conditions in Tokamaks, AIP conference proceedings 1237, 122 (2010).
[27] M. Siccinio, E. Fable, K. Lackner, A. Scarabosio, R. P. Wenninger and H Zohm, A 0D stationary model for the evaluation of the degree of detachment on the divertor plates, Plasma Physics and Controlled Fusion 58 (2016), 125011 (10 pp).
[28] G. A. Bird, Molecular gas dynamics and the direct simulation of gas flows, Clarendon Press, 1994.
[29] N. M. Laurendeau, Statistical Thermodynamics, Cambridge University Press, 2005.